Korean J. Chem. Eng., 34(1), 66-72 (2017)
DOI: 10.1007/s11814-016-0246-8

pISSN: 0256-1115
eISSN: 1975-7220

Synthesis of γ-alumina nano powder from Nepheline syenite

Mehran Chitan*,, Seyed Ali Hosseini***,†, Dariush Salari*, Aligholi Niaei**, and Habib Mehrizadeh*,****

*Research Laboratory of Petroleum Technology, Faculty of Chemistry, University of Tabriz, Tabriz, Iran
**Research Laboratory of Reactor and Catalyst, Faculty of Chemical Engineering, University of Tabriz, Tabriz, Iran
***Department of Chemistry, Faculty of Science, Urmia University, Urmia, Iran
(*Received 26 April 2016 • accepted 29 August 2016*)

Abstract−Nano γ-alumina was produced using Nepheline syenite ore by leaching and precipitation process at a certain pH in the presence of sodium dodecyl sulfate (SDS) as a surfactant. The produced nanostructure was characterized by XRD, SEM, EDX, DLS, BET and FT-IR. The XRD pattern confirmed the tetragonal structure of alumina The nano structure of alumina was approved by SEM and the particle size distribution were between 41 to 486 nm, confirmed by DLS. BET analysis showed that the specific surface area of nanopowder was about 39.1 m^2/g. The synthesis conditions were modeled and optimized by RSM. The optimum conditions resulted in leaching time, the mass ratio of Nepheline/HCl, and the reflux temperature of 2 h, 20, and 70 °C, respectively. Under optimum conditions, the extraction efficiency was 82%. The prepared nano γ-alumina has higher removal efficiency than commercial types in the removal of p-nitrophenol by adsorption process.

Keywords: γ-Alumina, Nanostructure, Hydrometallurgy, Nepheline Syenite, RSM, Adsorption

INTRODUCTION

Aluminum oxide, an inorganic compound with the chemical formula of Al_2O_3 [1], is used extensively because of its high melting point, uniform channels, high surface area, uniform pore size distribution and high heat resistance and applied as adsorbents, catalysts, planting, biological basis [2,3]. Specially, alumina due to the pore structure, high thermal resistance, good dispersion and the optimal price is used as a catalyst and base catalyst in the chemical industries [4]. Alumina consists of many thermodynamic phases such as γ, δ, θ, those finally transform to α phase with rising temperature [4,5]. The γ-alumina is the most important structure of the alumina that is widely used, such as a catalyst in the oil industry, composite structures for aerospace coatings and also used as insulation and thermally stable materials [6]. The γ-alumina is extensively used in the catalyst industry because of its high surface area and also the Lewis acid centers on its surface [7]. The alumina can be prepared in the laboratory with high purity from the aluminum nitrate and alkoxy aluminum precursors by hydrothermal, sol-gel, chemical deposition and micro-emulsion methods [8-11]. Nepheline syenite is an igneous rock, which is similar in its medium to coarse-grained granite [12]. The formula of Nepheline syenite is $Na_3KAl_4Si_4O_{16}$ and its essential composition is silica and also has a higher proportion of the alkalis, sodium, and potassium, as well as a higher proportion of alumina [12]. The alumina content of Nepheline syenite approximately is 25% [12]. Therefore, the Nepheline syenite ore, because of easy access, low cost and lack of mineral waste, is used as the raw material of alumina [12]. Different mesoporous alumina can be obtained by using various types of surfactants, and these surfactants act as templates [13]. For example, Triton X-100, and CTAB are used to produce nanostructure alumina from kaolin [13]. Sodium dodecyl sulfate (SDS) is an anionic surfactant that is used for synthesis alumina nanotubes from aluminum nitrate [14]. It is also used to modify the surface of alumina [15].

In this project, the nanostructure γ-alumina was produced via purification and precipitation method from Nepheline syenite ore, and the sodium dodecyl sulfate (SDS) was used as a surfactant to keep their nanostructure. Before the separation of the alumina precursor at the certain pH, the impurities of solute were removed by the precipitation of hydroxide. Response surface methodology (RSM) was used to study the effects of factors in the production process such as the leaching time, the mass ratio of Nepheline/HCl, and the reflux temperature and the extraction efficiency were considered as the desired response. The catalytic activity of prepared nano γ-alumina was examined in the removal of p-nitrophenol by adsorption process and compared with commercial types.

MATERIALS AND METHOD

1. Materials

The raw powders of Nepheline syenite were obtained from Azarshahr, Iran. The chemical composition of Nepheline syenite is presented in Table 1. Sodium dodecyl sulfate (SDS), hydrochloric acid, p-nitrophenol, and sodium hydroxide were analytical grade without further purification and obtained from Merck Co., Germany.

2. Synthesis of Nano γ-Alumina

The nano γ-alumina was produced using Nepheline syenite ore by leaching and precipitation. First, nepheline syenite ore was leached

†To whom correspondence should be addressed.
E-mail: seyedali.ho@gmail.com, s_ali_hosseini@yahoo.com

Table 1. Chemical composition of nepheline syenite

Component	Content
SiO_2	55.51
Al_2O_3	19.26
Fe_2O_3	2.42
MgO	1.32
TiO_2	0.41
CaO	4.18
Na_2O	5.3
K_2O	7.95
LOI	15.36

with the 6 M HCl solution with the 1 : 20 weight ratio of nepheline syenite to HCl under 2 h stirring at 70 °C. The suspension was filtered and the solute that contains aluminum cation was collected for the synthesis of aluminum hydroxide. NaOH solution (5 M) was added into the solute until the $AlCl_3$ completely transformed into $NaAlO_2$ at the pH upper than 9. In this range of pH, some impurity elements (such as Fe^{3+}, Na^+, K^+) precipitated and separated from the solute by filtering. The pH of the solute that contains $NaAlO_2$ was decreased to 7 by adding HCl solution (6 N) with the magnetic stirring until the alumina was precipitated completely in the form of boehmite. The precipitate was collected by centrifuge and washed with ethanol. The obtained precipitate was added to 50 mL of deionized water containing 0.5 g of SDS with vigorous stirring at 60 °C for 1 h to prevent particle aggregation and agglomeration. The suspension was aged for 48 h at room temperature and then the final white products were collected by filtration. The collected sample was washed with ethanol and dried at 100 °C. Finally, the as-synthesized samples were calcined at 750 °C for 3 h. The related reactions are presented below:

$$\text{Nepheline syenite}+HCl \rightarrow\rightarrow (Al^{3+}+Fe^{3+}+Na^+ +K^+ +\ldots) \quad (1)$$

$$(Al^{3+}+Fe^{3+}+Na^+ +K^+ +\ldots)+NaOH \rightarrow\rightarrow NaAlO_2+Na^+ +K^+ +Fe(OH)_3\downarrow (pH>9) \quad (2)$$

$$NaAlO_2+Na^+ +K^+ +HCl \rightarrow AlO(OH)\downarrow (\text{Boehmite})+Na^+ +K^+ \ (pH\sim 7) \quad (3)$$

$$AlO(OH)+SDS \rightarrow\rightarrow Al_2O_3 \quad (4)$$

3. Characterization of Prepared γ-Alumina Nanoparticles

X-ray diffraction (XRD) pattern was used to study the crystalline phase and the average crystalline size of prepared alumina. The XRD analysis was by D500 Siemens XRD diffractometer. The average crystallite size of prepared γ-alumina nanocrystals was calculated by Debye-Scherer equation (Eq. (5)) [16]:

$$D=\frac{k\lambda}{\beta\cos\theta} \quad (5)$$

FTIR analysis was used to identify the bond structure of the prepared γ-alumina. The infrared spectrum of γ-alumina was analyzed by Fourier transform infrared device manufactured by Bruker (Germany, the Tensor 27). To study the surface morphology of prepared γ-alumina nanoparticles, the SEM and EDX analyses were taken using SEM (TESCAN MIRA3-FEG). The DLS analysis was used to determine the size distribution of particles in solution and suspension. The DLS analysis was done with Nanotrac Wave. The BET analysis was used to determine the specific surface area and pore size of prepared nano γ-alumina by a micro pore analyzer (ASAP 2010, USA). The specific surface area (SSA) was measured by N_2 adsorption on the surface of prepared γ-alumina in the partial pressure of 0 to 0.5, and the pore size was determined by analysis of adsorption branch of BJH model.

4. Experimental Design Method

The experimental design was used to obtain high efficiency of extraction of alumina from nepheline syenite ore. The response surface methodology combined with central composite design (CCD) with value $\alpha=\pm 1.68$ was used in the leaching process for modeling and optimization of operational parameters. Three operational parameters as the effective variables include the reflex time (2 to 18 hours), mass ratio of acid to ore (5 to 20) and reflux temperature (70 to 120 °C). The leaching test was designed based on the CCD response surface method with six repeat tests in the midpoint, six tests as axial tests and eight tests for cubic point tests, and the efficiency of alumina was measured for each test of RSM. The details of design tests by CCD are presented in Table 2. Based on the results, coefficients obtained by the software and quadratic following relationship were obtained between the response variable and independent variables:

$$y=\beta_0+\sum_{i-1}^{k}\beta_i X_i+\sum_{i=1}^{k}\beta_{ii}X_i^2+\sum_{i=1}^{k-1}\sum_{j=2}^{k}\beta_{ij}X_iX_j+\varepsilon \quad (6)$$

In this equation, Y represents the variable response as alumina extraction efficiency and x_i represent the test levels as variables to figure out the code.

5. Adsorption of Pollutants from Aqueous Solution by Prepared Nano γ-Alumina

For the study the adsorption properties of prepared nano γ-alumina, the p-nitrophenol and Acid Blue 9 was selected as probe molecules of organic pollutant, and their removal efficiency was studied by adsorption process. To study the adsorption properties of prepared nano γ-alumina, 0.1 g of alumina was added to 100 mL of the solution of pollutants with the concentration of 20 ppm at the constant stirring (500 rpm) in the room temperature. After

Table 2. RSM design matrix and the values of response

Factors		Levels and limits				
		+1.681	+1	0	−1	−1.681
Time reflex (hour)	X_1	18	14.7568	10	5.2432	2
Acid to ore ratio (L/S)	X_2	20	16.9595	12.5	8.0405	5
Temperature (°C)	X_3	120	109.865	95	80.135	70

30 min, the samples were withdrawn from the suspension and filtered to remove alumina from solution. The amount of remaining pollutants in each solution was obtained by a spectrophotometer (S2100 Diode Array Spectrophotometer). The removal percentage for each one was calculated based on the following equation:

$$X = \frac{C_o - C_t}{C_t} \quad (7)$$

where C_o is the initial concentration of pollutants and C_t is the remaining concentration of pollutants after 30 min adsorption.

The adsorption activity of the prepared nano γ-alumina was compared with three types of γ-alumina (Merck, HF 254 and Azarshahr Company) at the same condition.

RESULTS AND DISCUSSION

1. Characterization of Prepared γ-Alumina Nanoparticles

The XRD patterns of produced γ-alumina and Nepheline syenite Ore are shown in Fig. 1. Fig. 1(a) shows the XRD pattern of nano γ-alumina and four index peaks of γ-alumina were observed at 31.72, 37.34, 45.46 and 66.85° [17]. From JCPDS 00-029-0063, the crystal structure of prepared nano γ-alumina is cubic. From Debye-Scherrer formula the average crystalline size of produced nanocrystals was calculated as about 42 nm. Fig. 1(b) indicates the XRD pattern of nepheline syenite. From the XRD pattern of nepheline syenite, the peak around 28° indicates the quartz (SiO_2) phase and the around 34-35° is attributed to alumina phase [12,16]. The alumina phase in the nepheline syenite is important and the precursor to synthesize of γ-alumina extract from this portion.

The FT-IR analysis of the synthesized γ-alumina at the different calcination temperature is shown in Fig. 2. According to the infrared spectrum, four peaks are observed. The peaks in the region of 400-1,000 cm^{-1} were generally associated with the stretching vibration of Al-O bonds. The Al-O stretching modes of [ν-A1O_6] were found below 900 cm^{-1}, whereas the peak around 978 cm^{-1} corresponded with ν-AlO_4. Band in the 1,124 cm^{-1} is in the rela-

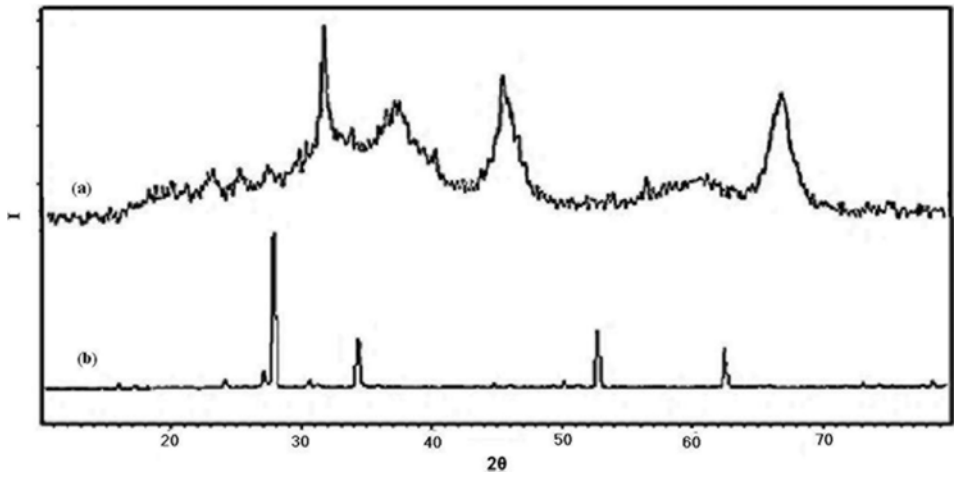

Fig. 1. The XRD pattern of (a) prepared nano γ-alumina (b) nepheline syenite ore.

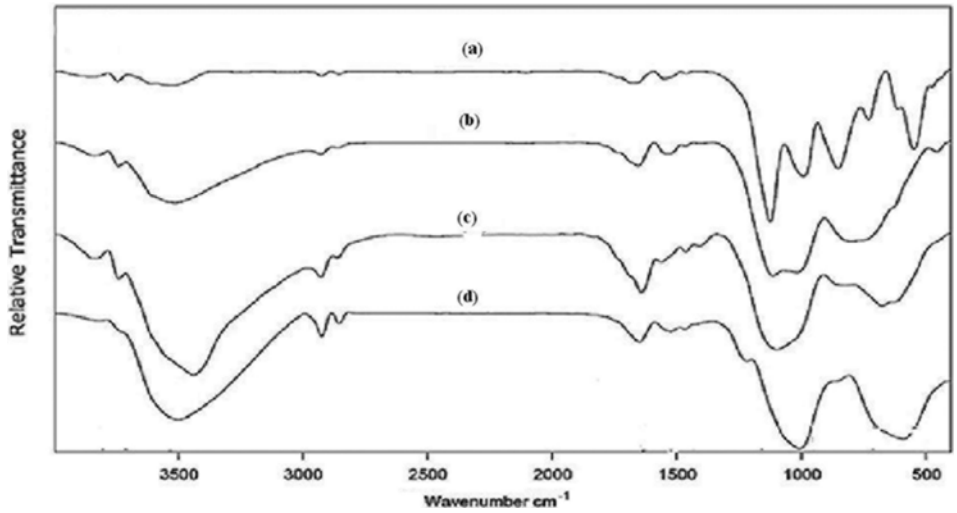

Fig. 2. The infrared spectrum of alumina calcined at different temperatures: (a) 750 °C, (b) 500 °C, (c) 250 °C and (d) the infrared spectrum of aluminum hydroxide.

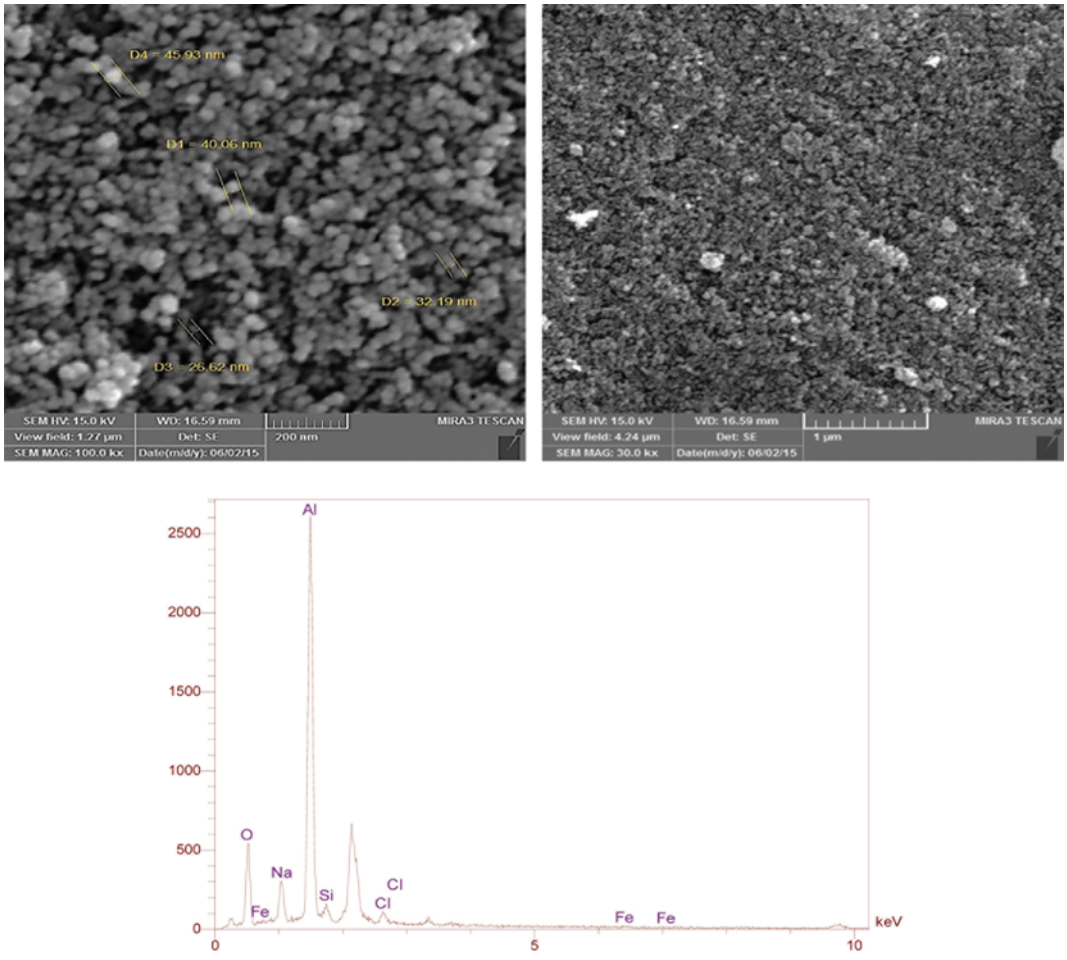

Fig. 3. (a) SEM images and (b) EDX spectrum of praperd nano γ-alumina.

tionship with symmetric stretch Al-OH. Peaks in the region of 1,400 cm^{-1} to 1,600 cm^{-1} are associated with the formation of alumina. The intensity of these peaks is reduced with increasing temperature and calcination that is attributed to the rapid growth of crystals of alumina nanoparticles [18]. The peaks around 3,500 cm^{-1} and 1,630 cm^{-1} were assigned to stretching and bending modes of adsorbed water [18]. In addition, the peaks in the 3,743 cm^{-1} and 3,854 cm^{-1} ranges are characteristic of γ-alumina [19,20]. In addition, from the FT-IR analysis, there is not any peak related to SDS structure and this is shown that with calcination the SDS was decomposed and removed from the alumina structure [21].

The SEM and EDX analyses of the synthesized γ-alumina are shown in Fig. 3. According to SEM image (Fig. 3(a)), the size of nanoparticles of the synthesized γ-alumina by sodium dodecyl sulfate (SDS) surfactant was in nano-scale range and particles are almost uniform with a spherical shape and the average size of nano particles is about 50 nm. The nano size and uniform morphology of the synthesized nanoparticles may be attributed to the surfactant role of SDS, and the surfactant acts as capping agent and causes the nano-size particles of γ-alumina [22]. According to the EDX spectrum and peak intensity of aluminum (Fig. 3(b)), it was observed that major portion of the synthesized nano γ-alumina is the Al. The EDX analysis and relative abundance of each element are presented in Table 3.

Table 3. Elemental composition of prepared nano γ-alumina

Elements	Al	O	Si	Na	Cl	Fe
Weight percent	49.49%	34.95%	4.45%	7.13%	3.41%	0.57%

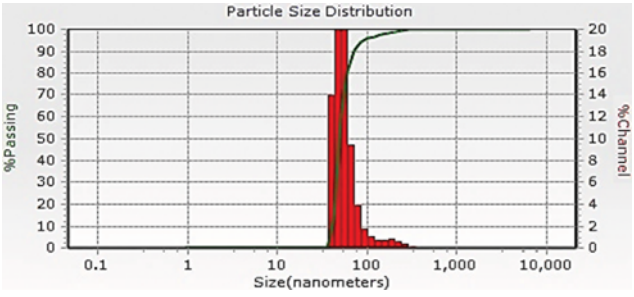

Fig. 4. DLS graph of nano γ-alumina prepared.

In addition, the relative distribution of particle size of the synthesized nano γ-alumina was determined by DLS analysis. The DLS graph is shown in Fig. 4. It is observed that the size distribution of nano γ-alumina particles was uniform and about 95% of the particles were in the range below than 100 nanometers, con-

Table 4. The results obtained from RSM

Test	Parameter values			Answers amounts	
	The reaction time	Mass ratio of acid to ore	The reaction temperature	The leaching percent obtained	Percent leaching predicted
	X_1	X_2	X_3		
1	10.0000	5.0000	95.000	13.5	19.2364
2	5.2432	16.9595	109.865	53.72	50.4857
3	14.7568	8.0405	80.135	16.75	19.0040
4	10.0000	20.0000	95.000	41.68	37.3298
5	10.0000	12.5000	95.000	29.00	29.8837
6	10.0000	12.5000	95.000	31.30	29.8837
7	10.0000	12.5000	120.000	56.30	62.5307
8	5.2432	16.9595	80.135	50.60	52.6898
9	2.0000	12.5000	95.000	26.80	32.7317
10	10.0000	12.5000	95.000	28.42	29.8837
11	5.2432	8.0405	109.865	37.60	30.7924
12	14.7568	8.0405	109.865	34.00	30.9300
13	5.2432	8.0405	80.135	43.40	40.5814
14	10.0000	12.5000	95.000	29.50	29.8837
15	14.7568	16.9595	80.135	15.00	20.8274
16	10.0000	12.5000	95.000	30.60	29.8837
17	10.0000	12.5000	95.000	30.72	29.8837
18	18.0000	12.5000	95.000	10.60	6.0545
19	14.7568	16.9595	109.865	38.50	40.3384
20	10.0000	12.5000	70.000	59.20	54.3556

Table 5. Results of analysis of variance (ANOVA) for the model

	Degrees of freedom	Sum of squares	Mean squares	F-value	P-value
Regression	8	3459.30	432.41	15.76	0.000
Linear	3	1334.91	444.97	16.22	0.000
Square	2	1806.96	903.48	32.93	0.000
Interaction	3	317.43	105.81	3.86	0.041
Lack of fit	6	295.55	49.26	39.22	0.000
Pure error	5	6.28	1.26		

firming the SEM analysis.

The BET analysis of the synthesized alumina was determined by N_2 adsorption. The specific surface area, pore volume, and pore diameter were 39.146 m^2/g, 4.820, and 4 nm, respectively. The surface area of the synthesized γ-Alumina is close to the surface area of alumina that was prepared in the presence of SDS surfactant by the other researchers [14].

2. Modeling and Optimization of Leaching Process by RSM

Response surface methodology (RSM) was applied to design the experiment and the statistical analysis of the process. The efficiency of the extraction of alumina in the leaching process is reported in Table 4. The following model (Eq. (8)) could best fit the experimental results among different evaluated models.

$$Y=499.3-4.17\,X_1+0.41\,X_2-9.64\,X_3-0.16X_1^2-0.03\,X_2^2+0.05\,X_3^2 -0.12\,X_1X_2+0.08\,X_1X_3+0.03\,X_2X_3 \quad (8)$$

The model predicted that the reaction time and temperature (X_1 and X_3) have a negative impact on the response, whereas the mass ratio of acid to ore (X_2) has a positive impact on the alumina production.

The results of analysis of variance (ANOVA) for the model are presented in Table 5. ANOVA is a statistical technique that subdivides the total variation in a set of data into component parts associated with specific sources of variation for the purpose of testing hypotheses on the parameters of the model [23]. Fisher's F-test was used to verify the statistical significance of the model. We concluded from the results of the F-test that the established model is statistically significant (i.e., ratio of mean square regression to mean square residual) with F-value of 15.76. In addition, the significance of the model was evaluated by the determination coefficient (R^2). The R^2 value means an acceptable agreement between the experimental and predicted values of the fitted data. Closeness of data and high value of the determination coefficient (R^2=0.92) shows the validity of the model [24,25].

The significance of the regression coefficient of the model terms was investigated by P-value and t-value. P-value and t-value of each

Table 6. Results of significance of the regression coefficient of the model terms

Term	Coef.	SE Coef.	T-value	P-value
Constant	29.42	1.81	16.22	0.000
Time	−7.93	1.42	−5.60	0.000
Ratio	5.38	1.42	3.79	0.003
Temperature	2.43	1.42	1.71	0.114
Time*Time	−3.65	1.37	−2.66	0.022
Temperature*Tempeature	10.15	1.37	7.39	0.000
Time*Ratio	−2.57	1.85	−1.39	0.192
Time*Temperature	5.43	1.85	2.93	0.014
Ratio*Temperature	1.90	1.85	1.02	0.328

term of the model are presented in Table 6. Conventionally, the larger t-value and smaller p-value ($p<0.05$) indicate the higher significance of the corresponding coefficient. The coefficients of the linear effect of time and mass ratio with a p-value of less than 0.05 were significant. In the case of quadratic effects of (X_{i2}), all effects except those of time*time (X_{12}) and Temperature*Temperature $(X_3)^2$ were significant at the confidence level of 95%, whereas the P-value of X_2^2 was higher than 0.05 and was removed from the model. In the case of binary terms, just the interaction of X_1X_3 was significant at the confidence level of 95% (p-value≤0.05) [26].

Pareto analysis is applied to determine the relative importance of each term of the model. Pareto analysis calculates the percentage effect of each term on the response, according to Eq. (3) and gives some information to interpret the results [27].

$$P_i=\left(\frac{b_i^2}{\Sigma b_i^2}\right)\times 100 \ (i\neq 0) \quad (9)$$

The results of Pareto analysis are shown in Fig. 5. The results suggest that the reflux time with a relative importance of 24.78% has the most important effect on the nano γ-alumina production. The Pareto analysis suggested that the order of relative importance of the factors is as follows: time>mass ratio of acid/Ore>temperature.

The purpose of RSM is to obtain the maximum extraction efficiency of nano γ-alumina and optimization of the parameters affecting the process. In this process, the optimum values of each parameter were obtained after testing the predicted by RSM. In which the optimum values were obtained for the time 2 h, mass ratio 20 times and temperature 70 °C, and by doing this the optimal values of maximum extraction rate will be 82% alumina.

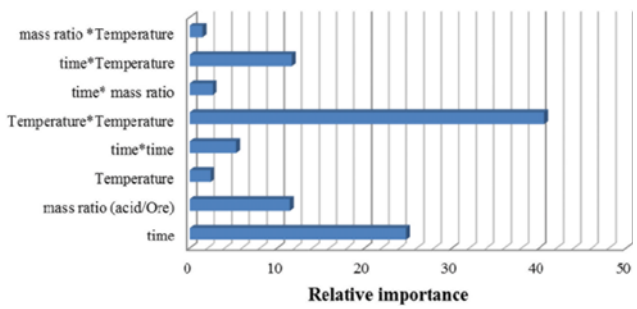

Fig. 5. Pareto chart analysis.

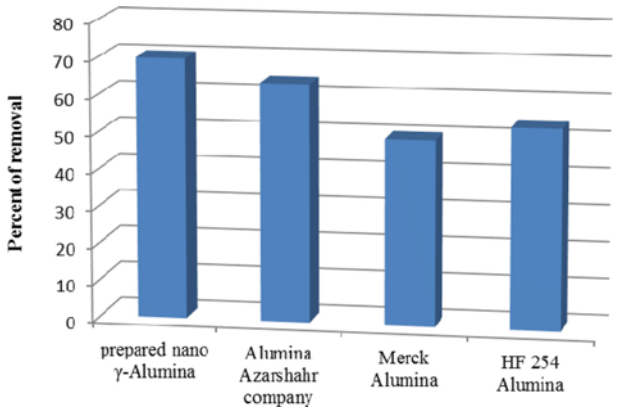

Fig. 6. The adsorption removal percentage of prepared nano γ-alumina and commercial nano γ-alumina; [P-nitrophenol]=20 ppm, [γ-alumina]=0.1 gr, pH=6.68 and temperature=27.5 °C.

3. Comparison of Adsorption Properties of the Synthesized Nano γ-Alumina with Commercial Alumina in Removal of p-Nitrophenol

Fig. 6 shows the removal percentage of p-nitrophenol and Acid blue 9 dye by the synthesized nano γ-alumina and commercial nano γ-alumina using the adsorption process. As shown, the removal percentage of p-nitro-phenol and Acid blue 9 by the synthesized nano γ-alumina is greater than the commercial types of nano γ-alumina. This high activity of nano γ-alumina may be attributed to uniform particles and the active site of nano γ-alumina. The higher adsorption property of nano γ-alumina can be related to the remaining impurities of Na^+ ions on the surface structure of nano γ-alumina. The Na^+ ions, remaining on the surface of nano γ-alumina, cause to increase surface protonated hydroxyls ($Al\text{-}OH_2^+$) and that causes to increase the adsorption capacity of nano γ-alumina [28,29]. In addition, it is well-known in literature that addition of Na^+ and other base metal cations on γ-alumina increases the heat of adsorption and consequently the adsorption intensity [25].

CONCLUSIONS

The nano γ-alumina in the cubic crystal structure with the average crystalline size of 42 nm and specific surface area of 39.1 m^2/g, was prepared successfully from Nepheline syenite ore in the presence of SDS as the surfactant at certain conditions. The effective parameters on the separation efficiency of γ-alumina from Nepheline syenite were modeled and optimized very well by RSM. A second-order model was successfully developed for the process by CCD of the RSM. Analysis of variance showed a high coefficient of determination value (R^2=0.921), thus ensuring a satisfactory adjustment of the second-order regression model with the experimental data. Pareto analysis revealed that the amount of the optimal conditions resulted in the reaction time, the mass ratio of acid to the ore and the reaction temperature of 2 h, 20 and 70 °C, where the efficiency resulted in 82%. The adsorption properties of the synthesized nano γ-alumina were higher than commercial type nano γ-alumina in the removal of aqueous pollutants, and this

higher activity was attributed to Na impurities on the surface of γ-alumina.

ACKNOWLEDGEMENTS

We especially thank the Iranian Nanotechnology Initiative Council for financial support.

REFERENCES

1. K. Davis, Material Review: Alumina (Al_2O_3), School of Doctoral Studies European Union Journal (2010).
2. F. Pan, X. Lu, T. Wang, Y. Wang, Z. Zhang, Y. Yan and S. Yang, *Mater. Lett.*, **91**, 136 (2013).
3. W. Li, Q. Jia, Z. Zhang and Y. Wang, *Korean J. Chem. Eng.*, **33**, 1337 (2016).
4. M. W. Tamele, *Discussions of the Faraday Society*, **8**, 270 (1950).
5. J. E. Park, B. B. Kim and E. D. Park, *Korean J. Chem. Eng.*, **32**, 2212 (2015).
6. S. Wang, X. Li, S. Wang, Y. Li and Y. Zhai, *Mater. Lett.*, **62**, 3552 (2008).
7. G. Paglia, A. L. Rohl, C. E. Buckley and J. D. Gale, *Phys. Rev. B*, **71**, 224115 (2005).
8. B. L. Cushing, V. L. Kolesnichenko and C. J. O'Connor, *Chem. Rev.*, **104**, 3893 (2004).
9. M. Niederberger and N. Pinna, *Metal oxide nanoparticles in organic solvents: synthesis, formation, assembly and application*, Springer Science & Business Media (2009).
10. K. Byrappa and M. Yoshimura, *Handbook of hydrothermal technology*, William Andrew (2012).
11. Y. Kim, B. Lee and J. Yi, *Korean J. Chem. Eng.*, **19**, 908 (2002).
12. S. A. Hosseini, *Int. J. Mater. Chem. Phys.*, **1**(2), 93 (2015).
13. F. Pan, X. Lu, T. Wang, Y. Wang, Z. Zhang and Y. Yan, *Appl. Clay Sci.*, **85**, 31 (2013).
14. L. Qu, C. He, Y. Yang, Y. He and Z. Liu, *Mater. Lett.*, **59**, 4034 (2005).
15. M. Ezoddin, F. Shemirani, K. Abdi, M. K. Saghezchi and M. Jamali, *J. Hazard. Mater.*, **178**, 900 (2010).
16. K. Parida, A. C. Pradhan, J. Das and N. Sahu, *Mater. Chem. Phys.*, **113**, 244 (2009).
17. N. Majidian, N. Habibi and M. Rezaei, *Korean J. Chem. Eng.*, **31**, 1162 (2014).
18. H. Yang, M. Liu and J. Ouyang, *Appl. Clay Sci.*, **47**, 438 (2010).
19. A. R. Ferreira, E. Küçükbenli, S. De Gironcoli, W. F. Souza, S. S. X. Chiaro, E. Konstantinova and A. A. Leitão, *Chem. Phys.*, **423**, 62 (2013).
20. T. H. Ballinger and J. T. Yates Jr., *Langmuir*, **7**, 3041 (1991).
21. L. Sicard, P. L. Llewellyn, J. Patarin and F. Kolenda, *Micropor. Mesopor. Mater.*, **44-45**, 195 (2001).
22. J. C. Ray, K.-S. You, J.-W. Ahn and W.-S. Ahn, *Micropor. Mesopor. Mater.*, **100**, 183 (2007).
23. M. Zabeti, W. M. A. W. Daud and M. K. Aroua, *Appl. Catal. A: Gen.*, **366**, 154 (2009).
24. M. N. Chong, H. Zhu and B. Jin, *Chem. Eng. J.*, **156**, 278 (2010).
25. X. Han, Y. He, H. Zhao and D. Wang, *Korean J. Chem. Eng.*, **31**, 1810 (2014).
26. W. Wang, H. Ma, W. Xu, L. Gong, W. Zhang and D. Zou, *Biochem. Eng. J.*, **39**, 604 (2008).
27. A. R. Khataee, M. Zarei and L. Moradkhannejhad, *Desalination*, **258**, 112 (2010).
28. L. Vordonis, P. G. Koutsoukos and A. Lycourghiotis, *Colloids Surf.*, **50**, 353 (1990).
29. J. Xiao, L. Zhao, W. Zhang, X. Liu and Y. Chen, *Korean J. Chem. Eng.*, **31**, 253 (2014).